Cell Reports
Physical Science

CellPress
OPEN ACCESS

Article

Production of β-ketoadipic acid from glucose in *Pseudomonas putida* KT2440 for use in performance-advantaged nylons

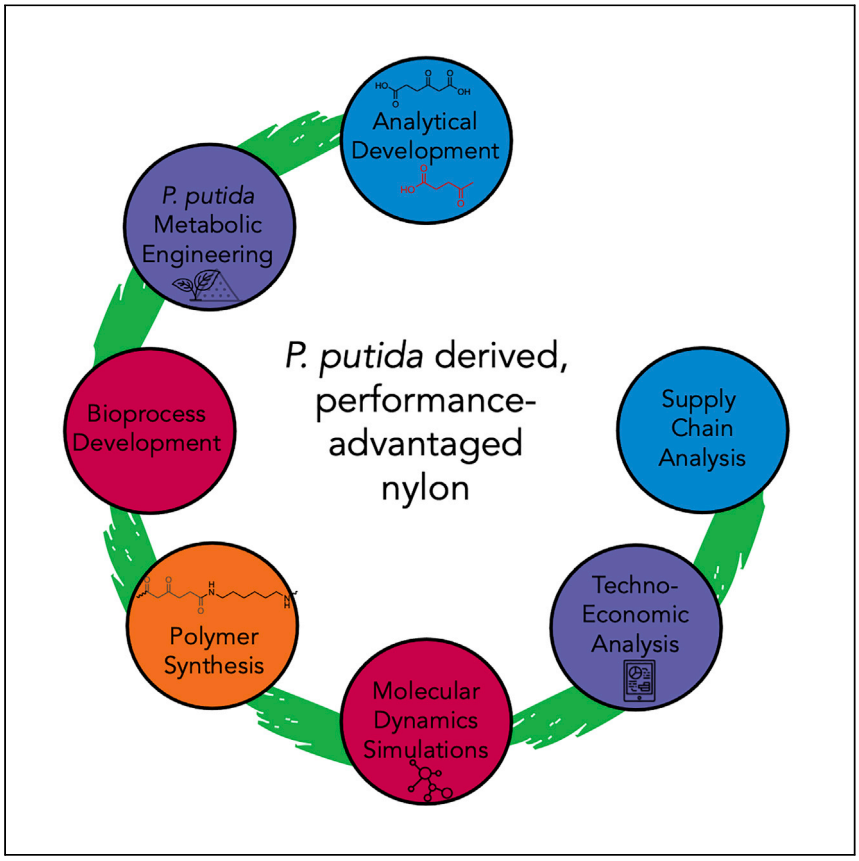

Rorrer et al. present an integrated process to biologically produce β-ketoadipic acid (βKA) from glucose and use this building block as a replacement for adipic acid. The incorporation of bio-derived βKA results in nylons with improved thermal properties alongside lower water permeability, associated supply-chain energy, and greenhouse gas emissions relative to nylon-6,6.

Nicholas A. Rorrer, Sandra F. Notonier, Brandon C. Knott, ..., Davinia Salvachúa, Michael F. Crowley, Gregg T. Beckham

gregg.beckham@nrel.gov

Highlights

Pseudomonas putida is engineered to produce β-ketoadipic acid (βKA) from glucose

βKA-nylon exhibits enhanced thermal properties and permeability over nylon-6,6

Computational results explain the molecular basis for improved βKA-nylon properties

Analysis suggests that βKA can be viably manufactured with improved sustainability

Rorrer et al., Cell Reports Physical Science *3*, 100840
April 20, 2022
https://doi.org/10.1016/j.xcrp.2022.100840

Cell Reports
Physical Science

CellPress
OPEN ACCESS

Article

Production of β-ketoadipic acid from glucose in *Pseudomonas putida* KT2440 for use in performance-advantaged nylons

Nicholas A. Rorrer,[1,5] Sandra F. Notonier,[1,5] Brandon C. Knott,[1,5] Brenna A. Black,[1,5] Avantika Singh,[2,5] Scott R. Nicholson,[3,5] Christopher P. Kinchin,[2] Graham P. Schmidt,[1] Alberta C. Carpenter,[3] Kelsey J. Ramirez,[1,4] Christopher W. Johnson,[1,4] Davinia Salvachúa,[1,4] Michael F. Crowley,[1] and Gregg T. Beckham[1,4,6,*]

SUMMARY

Biomass-derived chemicals can offer unique chemical functionality relative to petroleum-derived building blocks. To this end, here we report that β-ketoadipic acid (βKA), a C6 diacid with a β-ketone group, can be used as a performance-advantaged replacement for adipic acid in a nylon-6,6 analog. Building on our previous efforts to produce shikimate-derived products from carbohydrates, *Pseudomonas putida* KT2440 is engineered to produce βKA from glucose, achieving a 26 g/L titer. Following purification, βKA imparts an increase of 69°C above the nylon-6,6 glass transition temperature and 20% reduced water permeability, equivalent to nylon-6,10. Molecular simulations predict that the enhanced thermal properties result from rigidity introduced by the β-ketone. Process analysis predicts that βKA can be produced for US$1.94/kg from sugars, requiring 63% less energy and emitting 43% less greenhouse gases than fossil-based adipic acid. Overall, this study illustrates the potential for βKA to serve as a useful building block for bio-based polymers.

INTRODUCTION

The production of sustainable chemicals and materials from lignocellulose and other renewable feedstocks is a key component in reducing dependence on fossil carbon and mitigating the effects of climate change.[1–5] Many efforts to this end have focused on synthesis of "direct replacement" chemicals, which are chemically identical to compounds produced today from fossil sources.[6,7] However, the commercialization of bio-based direct replacement chemicals remains challenging, especially when competing with the mature petrochemical industry.

The challenging economics for bio-based direct replacement chemicals has prompted the bioproducts community, in part, to develop molecules that are chemically distinct from petroleum-derived building blocks and that offer advantageous properties.[8] The concept of "bioprivileged" molecules, from Shanks and Keeling, serves as a framework to examine biomass-derived chemicals that could fulfill both existing and emerging markets.[8,9] In parallel, the concept of performance-advantaged bioproducts was developed, defined by Fitzgerald and Bailey as "novel products where the bio-based product molecule does not resemble an existing petroleum-derived molecule in structure, but offers a

[1]Renewable Resources and Enabling Sciences Center, National Renewable Energy Laboratory, Golden, CO 80401, USA

[2]Carbon Catalytic Transformation and Scale-Up Center, National Renewable Energy Laboratory, Golden, CO 80401, USA

[3]Strategic Energy Analysis Center, National Renewable Energy Laboratory, Golden, CO 80401, USA

[4]Agile BioFoundry, Emeryville, CA 94608, USA

[5]These authors contributed equally

[6]Lead contact

*Correspondence: gregg.beckham@nrel.gov

https://doi.org/10.1016/j.xcrp.2022.100840

performance advantage over existing products."[10,11] Performance advantages can occur anywhere along a supply chain, from sourcing, manufacturing, use, to end-of-life.[12]

Aligned with the concept of performance-advantaged bioproducts, plant-based feedstocks including carbohydrates and lignin-derived compounds inherently contain oxygen functionality, differing from fossil-based hydrocarbons. Moreover, transformations of carbohydrates and lignin-derived intermediates via synthetic biology, chemical catalysis, and the combination thereof can offer bio-based chemicals that differ from fossil-based compounds.[7,9,13–18] From a biological perspective, metabolic pathways across the kingdoms of life offer many potential compounds for exploration as performance-advantaged bioproducts.[12,13] Among various regions of metabolic space, molecules from the shikimate pathway have been studied as precursors to adipic acid and terephthalic acid via chemo-catalytic conversion of *cis,cis*-muconic acid (MA) and can be produced from biomass-derived sugars.[19–27] Recently, MA has been used directly in biopolymers[12,28–30] or as a precursor to new molecules.[21,31,32] Additionally, lignin-derived aromatic compounds can also be biologically converted into MA.[21,22,26,27,33–35]

Beyond MA, there are other compounds of interest downstream of oxidative aromatic ring-opening reactions from the central intermediates protocatechuate (PCA) and catechol, including β-ketoadipate (βKA), among others.[36–39] These molecules, derivable from *Pseudomonas putida*, have been demonstrated to be applicable to a wide variety of applications such as nylons, polyurethanes, and polyesters.[21,23,28–30,39–41] In 2019, we reported the metabolic engineering of 16 *P. putida* KT2440 strains to produce all 16 known intermediates between PCA and catechol and central carbon metabolism.[39] Of interest here, we demonstrated a βKA titer of 40 g/L from an aromatic substrate. We also showed that βKA, when substituted for adipic acid in nylon-6,6, imparts a higher glass transition temperature (T_g). In the same study, we achieved a molar yield of MA from glucose of 38% via the shikimate pathway. Subsequently, we improved the productivity of MA production from glucose from 0.07 g/L/h to 0.21 g/L/h by deletion of the transcriptional repressor gene, *hexR*, in *P. putida*.[42] Taken together, these previous results indicate that βKA is a potentially promising platform molecule to pursue via these metabolic pathways to produce performance-advantaged bioproducts from sugars.

Here, we build on previous work[39,42] to demonstrate that βKA can serve as an adipic acid and sebacic acid replacement in performance-advantaged nylons. We engineer *P. putida* strains to convert glucose to βKA at bioprocess metrics relevant for polymerization. Given the propensity of βKA to decarboxylate, an accessible method for high-performance liquid chromatography (HPLC)-based quantitation of βKA was developed. Multiple nylon-6,6 formulations with βKA in place of adipic acid were synthesized and their properties compared with those of nylon-6,6 from adipic acid and hexamethylenediamine (HMDA) and nylon-6,10 from sebacic acid and HMDA. The improved thermal properties of the βKA-based nylon were rationalized using molecular dynamics (MD) simulations. Techno-economic analysis (TEA) and supply-chain modeling using Materials Flow through Industry (MFI)[43] were conducted to estimate the cost drivers and sustainability improvements relative to fossil-based adipic acid and bio-based sebacic acid. Overall, this work demonstrates that βKA can enable performance-advantaged nylon production, with potentially beneficial economics and lower supply-chain energy and greenhouse gas (GHG) emissions relative to diacids used today.

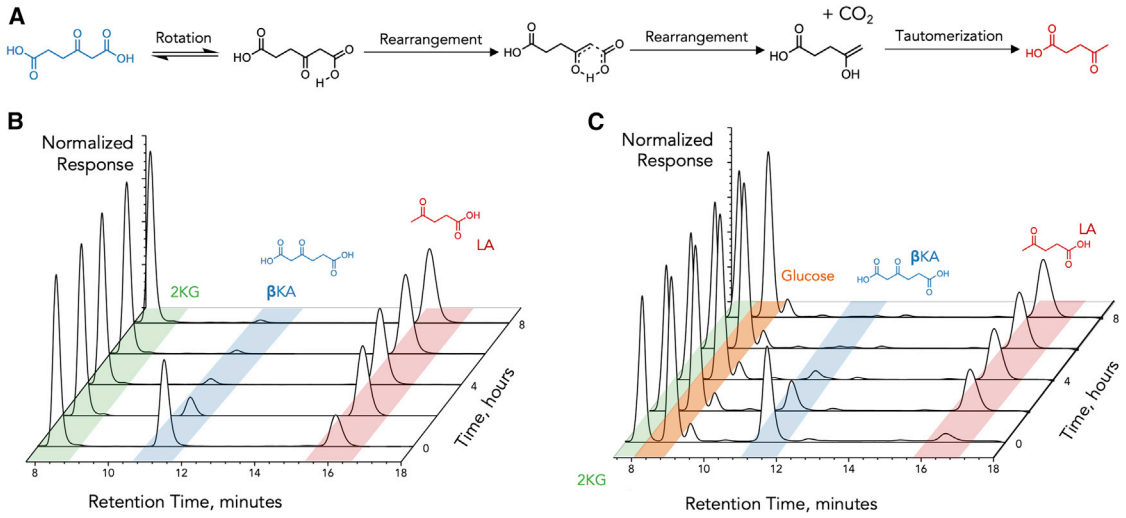

Figure 1. HPLC method development for βKA quantification

(A) Decarboxylation mechanism of βKA (blue) to levulinic acid (LA, red).

(B) Liquid chromatography (LC)-refractive index detector (RID) chromatograms demonstrating decarboxylation of βKA as a function of time with authentic standards at a concentration of 1 g/L. The theoretical maximum of 0.72 g/L LA was reached after 4 h of reaction at 50°C, while glucose and 2-ketogluconate were unaffected upon heating with sulfuric acid.

(C) LC-RID chromatograms demonstrating the decarboxylation of βKA as a function of time with an authentic biological sample derived from *P. putida* CJ390 (vide infra) with a βKA spike addition to show lack of matrix effect on separations, limited interaction between key analytes, and specificity of the method for LA. Decarboxylation to LA may occur during fermentation but is not detected by this technique or other documented techniques in the literature;[38,39] however, as decarboxylation occurs upon βKA reconstitution (Figure S1) it may occur in fermentation media. 2KG, 2-ketogluconate; βKA, β-ketoadipic acid; LA, levulinic acid.

RESULTS

Analytical method development for βKA quantification

A reliable analytical method to quantify βKA was first developed to overcome the challenges associated with decarboxylation of βKA to levulinic acid (Figure 1A).[38] Previous work demonstrated that βKA conversion to levulinic acid is accelerated upon heating (e.g., derivatization reactions or gas chromatography analysis) or pH < 7 (e.g., contact with acidic mobile phases during HPLC analysis).[39] To overcome this limitation, previous HPLC analysis of βKA employed an alkaline mobile phase that resolved the aromatic substrate from βKA without decarboxylation of βKA to levulinic acid. Despite the capability of this technique to quantify βKA produced from aromatic compounds, it is not applicable here owing to the co-elution with glucose. Therefore, a more universal method was developed to track and differentiate feedstock consumption, metabolite concentrations, and product formation without the use of an authentic βKA standard for quantitation.

The method reported here converts βKA into levulinic acid (Figure 1A) via heating in the presence of sulfuric acid, so that levulinic acid can be quantified and calculated back to βKA in a 1:1 M ratio. By converting βKA to levulinic acid, an acidic mobile phase can be implemented to obtain separation of key metabolites. This method is applicable when levulinic acid is not biologically produced within the pathway. Initial screening studies revealed that sulfuric acid was both compatible with the ion-exclusion chromatography utilized and effective at converting βKA to levulinic acid (Figures 1B and 1C). Glucose and other metabolites analyzed in this work (e.g., 2-ketogluconate) were not affected by sulfuric acid (Figure 1C). Validation studies are shown in Figures S1–S3 and Tables S1 and S2. The method was deemed

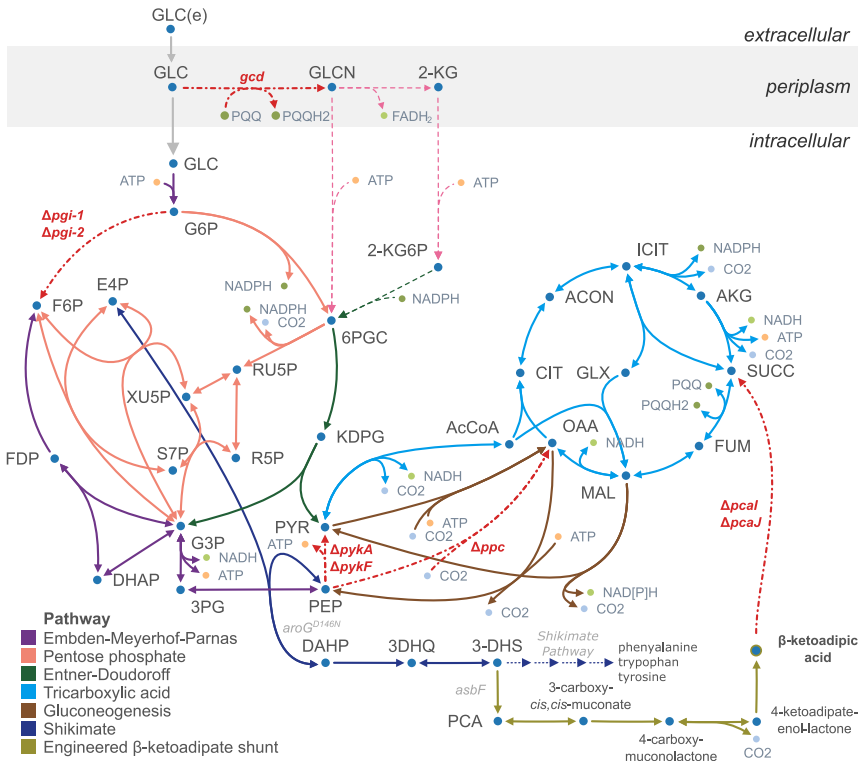

Figure 2. Metabolic pathway for conversion of glucose to βKA in the engineered *P. putida* strain SN301

Deleted genes are labeled in red and enzymatic reactions eliminated by those deletions are indicated by dotted red arrows. Deletion of *gcd*, *pgi-1*, *pgi-2*, *pkyA*, *pykF*, and *ppc* limit growth on glucose and promote availability of E4P and PEP, which are condensed to enter the shikimate pathway via an exogenous, feedback-resistant DAHP synthase encoded by $aroG^{D146N}$. An exogenous dehydratase encoded by *asbF* converts 3-DHS to PCA that is metabolized via the native pathway to generate βKA, which accumulates rather than being metabolized further due to the deletion of *pcaIJ*. Abbreviations of key metabolites are as follows: GLC, glucose; GLCN, gluconate; 2-KG, 2-ketogluconate; E4P, erythrose 4-phosphate; PYR, pyruvate; PEP, phosphoenolpyruvate; DAHP, 3-deoxy-D-arabino-heptulosonate-7-phosphate; 3-DHS, 3-dehydroshikimate; PCA, protocatechuate. Full names of all metabolite abbreviations can be found in Table S3.

accurate and reliable, and therefore implemented to analyze all subsequent experiments presented in this work. Further details are provided in supplemental experimental procedures.

Metabolic engineering and bioprocess development to produce βKA

P. putida KT2440 was employed as a host for βKA production because of its inherent robustness and native β-ketoadipate pathway.[44–46] In *P. putida*, glucose is metabolized via the EDEMP cycle, comprising the Entner-Doudoroff (ED), pentose phosphate (PP), and gluconeogenic Embden-Meyerhof-Parnas (EMP) pathways.[47] To engineer a strain to convert glucose to βKA (Figure 2), a gene encoding the 3-dehydroshikimate dehydratase from *Bacillus cereus*, AsbF, was introduced to convert 3-dehydoshikimate, an intermediate in the shikimate pathway for aromatic amino acid biosynthesis, to PCA, which is metabolized via the βKA pathway.[19,39] This gene was integrated in place of the genes encoding PcaIJ, the β-ketoadipate coenzyme A transferase, causing βKA to accumulate and resulting in the strain CJ390 (Tables 1 and S4–S6).

Table 1. Strains used in this study

Strain	Genotype
CJ390	*P. putida* KT2440 Δ*pcaIJ*::Ptac:*asbF*
SN4	*P. putida* KT2440 Δ*pykA*::Ptac:*aroG-D146N*:*asbF* Δ*pykF* Δ*ppc* Δ*pgi-1* Δ*pgi-2* Δ*pcaIJ*
CJ601	*P. putida* KT2440 Δ*pykA*::Ptac:*aroG-D146N*:*asbF* Δ*pykF* Δ*ppc* Δ*pgi-1* Δ*pgi-2* Δ*pcaIJ* Δ*gcd*
SN301	*P. putida* KT2440 Δ*pykA*::Ptac:*aroG-D146N*:*asbF* Δ*pykF* Δ*ppc* Δ*pgi-1* Δ*pgi-2* Δ*pcaIJ* Δ*gcd* Δ*hexR*

Previously a set of genetic modifications was identified to increase carbon flux to MA,[39,42] which is also derived from PCA, and those were similarly applied here. Specifically, the condensation of phosphoenolpyruvate (PEP) and erythrose 4-phosphate to form 3-deoxy-D-arabino-heptulosonate-7-phosphate (DAHP) is the first committed step in the shikimate pathway and is subject to feedback inhibition, so a gene encoding a feedback-resistant DAHP synthase from *Escherichia coli* ($AroG^{D146N}$) was introduced.[48] The genes *pykA*, *pykF*, and *ppc* were deleted to prevent PEP from entering the tricarboxylic acid cycle, instead allowing it to be routed to the shikimate pathway. The genes *pgi-1* and *pgi-2* were deleted to interrupt the ED-EMP cycle, which can otherwise cycle to generate pyruvate for growth independent of PEP, generating strain SN4. To prevent the conversion of glucose to gluconate and 2-ketogluconate, which can accumulate as a by-product in engineered strains,[39] *gcd* was deleted, resulting in strain CJ601. Finally, the gene encoding HexR, a transcriptional repressor of genes encoding enzymes in the glycolytic part of the EDEMP cycle, was deleted[42,49] to generate strain SN301.

The performance of strains CJ390, SN4, CJ601, and SN301 was compared in bioreactors in fed-batch mode at an initial glucose concentration of 15 g/L (Figures 3A, 3B, and S4). After the batch phase, glucose levels were maintained between ~2 and 15 g/L by constantly feeding a solution containing glucose and ammonium sulfate during the fed-batch phase. The glucose feeding ceased when glucose utilization was negligible. The genetic modifications in SN4 allowed for an increase in βKA titers, metabolic yields, and productivities by 8-fold, 7-fold, and 9-fold, respectively, compared with the base strain, CJ390 (Figures 3A and 3B). However, both strains (SN4 and CJ390) accumulated high concentrations of 2-ketogluconate (>100 g/L) (Figures S4A and S4B) and small amounts (<3.5 g/L) of gluconate—a metabolic intermediate between glucose and 2-ketogluconate (Figure 2)—and βKA production did not exceed 7 g/L in these two strains. The deletion of *gcd* in CJ601 eliminated the accumulation of both 2-ketogluconate and gluconate and increased the yield of βKA from 0.06 to 0.25 mol/mol, compared with SN4 (Figure 3B). The deletion of *gcd* also led to substantially reduced growth rates (Figures S4B and S4C). Lastly, the deletion of *hexR* in CJ301 was key to improving growth rates (Figures S4C and S4D) and improving βKA titer, metabolic yield, and productivity. Specifically, the titer increased to 17 g/L, the yield to 0.36 mol/mol, and the rate to 0.093 g/L/h in SN301 compared with those achieved in CJ601 under the same conditions (7.9 g/L, 0.25 mol/mol, and 0.033 g/L/h) (Figures 3A and 3B).

The best-performing strain, SN301, was further evaluated in different cultivation conditions aimed at optimizing conversion at larger scale (Figures S4D–S4F and S2). First, we changed the base used for pH controls (NH_4OH instead of NaOH). NH_4OH exhibits lower environmental impacts relative to NaOH based on life-cycle assessment (LCA, vide infra). As detailed in supplemental experimental procedures, NaOH emits 1.3 kg CO_2-e/kg in its manufacture while NH_4OH emits 0.3 kgCO_2-e/kg. In addition,

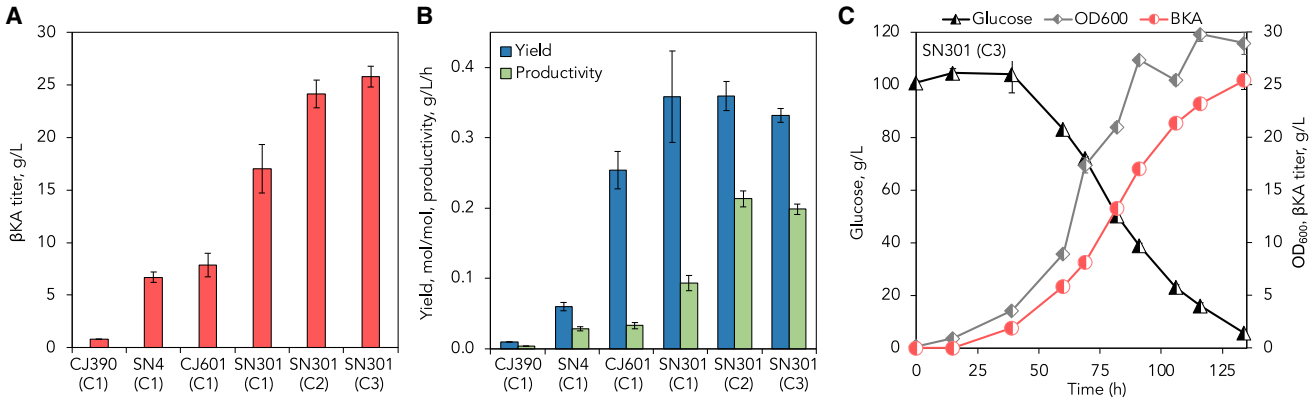

Figure 3. βKA production from glucose by engineered *P. putida* strains in bioreactors

(A) βKA titers (g/L), (B) βKA metabolic yields (mol βKA/mol glucose) and productivities (g/L/h), and (C) time-course profiles for bacterial growth, glucose utilization, and βKA production for the cultivation of SN301 in batch mode. C1: condition 1, fed-batch cultivation that includes a 1 L batch volume, initial 15 g/L glucose, inoculation with washed cells, and pH control with 4 N NaOH. C2: condition 2, fed-batch cultivation that includes a 1.5 L batch volume, initial 15 g/L glucose, inoculation with non-washed cells, and pH control with 4 N NH_4OH. C3: condition 3, batch cultivation that includes a 1.5 L batch volume, initial 100 g/L glucose, inoculation with non-washed cells, and pH control with 4 N NH_4OH. See supplemental experimental procedures for additional information on the cultivation conditions. All cultivations were conducted in duplicate experiments, excluding CJ601 and CJ390, which were conducted in triplicate and singlet, respectively. Results show the average values. Error bars represent the absolute difference between duplicates or the SD in triplicates. Time-course glucose utilization data are provided in Figure S5.

NH_4OH replaces the inorganic nitrogen source previously used. Second, cells from the seed culture were directly transferred into the bioreactors without washing, which is more process relevant.[39] Third, the initial batch volume was increased from 1 L to 1.5 L to reduce the shear stress of the impellers on the cells on the surface of the medium. These new conditions were also tested in batch mode (with an initial glucose concentration of 100 g/L) (Figure 3C), in addition to fed-batch mode (Figures S4A–S4D). Overall, the results in both batch and fed-batch mode in the optimized cultivation conditions were similar (Figures 3A, 3B, S4E, and S4F). βKA productivities increased over 2-fold (0.21 g/L/h) compared with the initial cultivation conditions in SN301 (0.09 g/L/h), and yields remained relatively constant (0.33–0.36 mol βKA/mol glucose) (Figure 3B). Ammonium levels were also tracked in all the cultivations (Figure S4). The results showed that the use of NH_4OH is also sufficient to serve as a nitrogen source to the cells (Figures S4E and S4F). Further information on strain development and bioreactor cultivations can be found in supplemental experimental procedures. With these results, batch cultivations under the optimized conditions (Figure 3C) were used to produce βKA for polymerization experiments.

Polymerization of βKA into a nylon-6,6 analog

Due to the similarity of adipic acid and βKA, nylon-6,6 was selected as the primary polymer to study the effect of βKA incorporation. Polymerization was conducted either via melt polymerization of the diacid acyl chlorides with HMDA or via melt polymerization of the HMDA-carboxylate salt. The acyl chlorides are primarily reported in this work as their use avoids imine formation and βKA decarboxylation; however, the salt polymerization was also conducted as a proof of concept owing to its industrial relevance and for subsequent TEA/LCA modeling. The salt polymerization further ensures an equimolar amount of amine and carboxylic acid while not exhibiting signs of decarboxylation. Acyl chlorides were prepared by the reaction of the diacids with phosphorous oxychloride.

For the polymerization of adipic acid with HMDA, the resulting polymer is equivalent to commercial nylon-6,6,[50] exhibiting the typical nylon-6,6 T_g of 62°C and melting

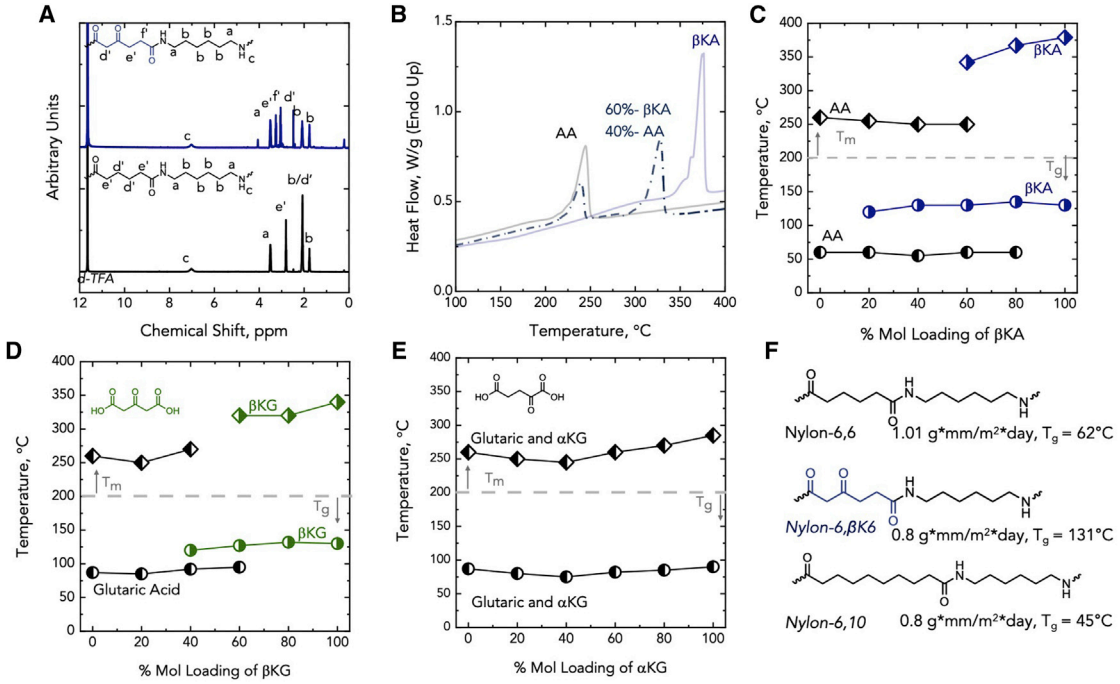

Figure 4. Properties of ketone-containing copolymers

(A–E) (A) NMR spectra, (B) DSC trace of homopolymers and copolymers, and (C) thermal properties of the βKA and adipate homopolymer and copolymers. Additional thermal properties of the (D) βKG and (E) αKG nylon blends as a function of ketone-diacid loading.

(F) Water permeabilities, T_g values, and structures of nylon homopolymers. The permeability of nylon-6,6 and nylon-6,βK6 was reported previously.[39] Table S8 provides numerical data for (C), (D), and (E). d-TFA, deuterated trifluoroacetic acid; βKG, β-ketoglutarate; αKG, α-ketoglutarate.

temperature (T_m) of 252°C. The synthesis of the βKA homopolymers has been previously reported and was replicated here,[39] where the βKA and HMDA polymer (nylon-6,βK6 hereafter) exhibited a T_g of 131°C and T_m of ~380°C. Notably, nylon-6,βK6 degraded near its T_m. The nuclear magnetic resonance (NMR) spectra for nylon-6,6 and nylon-6,βK6 are shown in Figure 4A and differential scanning calorimetry (DSC) traces in Figure 4B, alongside a co-polymer trace. The NMR spectra demonstrate no enol formation during polymerization. Table S7 provides further polymer characterization including molecular weight, polydispersity index (PDI), onset of thermal degradation, and characterization of the nylons polymerized from salts. Supplemental experimental procedures describe the polymer characterization techniques.

Copolymers of the nylon-6,6 and nylon-6,βK6 were subsequently synthesized to further examine the effect of the β-ketone by mixing adipoyl chloride (the acyl chloride of adipic acid) and the acyl chloride of βKA at molar loadings of 0%, 20%, 40%, 60%, 80%, and 100% (βKA homopolymer). The resulting copolymers exhibited molecular weights on the order of 30 kDa with a PDI near 2.0 (Tables S7 and S8), indicating the formation of copolymers instead of the formation of a polymer blend. Interestingly, the βKA copolymers exhibited two distinct thermal regimes, which can be potentially attributed to block regions of the βKA-HMDA and the adipate-HMDA polymers (Figures 4B and 4C).[51] These results suggest that the β-ketone in βKA leads to an arrestment of the kinetic mobility of the polymer chain, hence the higher T_g, and possibly greater intermolecular interactions between ketones and carbonyls, hence the higher T_m.

To further evaluate the effect of the ketone group on polymer properties, homopolymers and copolymers of HMDA with glutaric acid and β-ketoglutaric acid (βKG), or with glutaric acid and α-ketoglutaric acid (αKG), were produced with the same procedure. βKG and αKG were selected because they could be purchased commercially. The nylon-5,6 glutaric acid-based homopolymer exhibited a T_g higher than nylon-6,6 and a comparable T_m. The βKG copolymers exhibited behavior similar to that of the βKA copolymers, in which two distinct T_g values are observed, which we again attribute to the block regions and that the β-ketone results in an elevated T_g (Figure 4D). Conversely, the αKG copolymers did not exhibit a higher T_g than nylon-5,6 and displayed slight eutectic behavior as observed by a T_g minimum at 40% loading (247°C and 79°C, respectively) in Figure 4E.

As previously reported, βKA-based nylons exhibited reduced water permeability relative to nylon-6,6. For this property specifically, the βKA nylons were also compared with nylon-6,10. Nylon-6,10 is known to exhibit reduced water permeability and uptake relative to nylon-6,6 and is synthesized from HMDA and sebacic acid,[52,53] the latter of which can be obtained from castor oil. Here, nylon-6,10 was polymerized for comparison with both nylon-6,6 and nylon-6,βK6 by the melt polymerization of both the acyl chloride of sebacic acid with HMDA and the respective amine-carboxylate salt (salt polymerization data are provided in Table S7). The nylon-6,10 polymer exhibited a T_g of 45°C and a 20% reduction in water permeability (Figure 4F) relative to nylon-6,6, which is the same reduction achieved with the βKA-based nylons. Overall, the polymer characterization data indicate that the β-ketone imparts favorable behavior to polyamides relevant to their commercial applications.

Molecular simulation of nylons

MD simulations were conducted to investigate the molecular-level effect of the β-ketone group on the polymer backbone flexibility and hydrogen-bonding patterns. Polymer rigidity was examined by estimating the probabilistic configuration (quantified via the dihedral angles) and correlation times of backbone carbons as a function of ketone placement. More flexible polymer segments will exhibit shorter correlation times and sample a wider variety of configurations while more rigid polymer segments will possess longer correlation times and sample fewer configurations.

To these ends, we simulated nylon-6,6, nylon-6,αK6, and nylon-6,βK6 with the CHARMM36 force field[54] and additional force field parameters generated via CGenFF (Figure S6; Tables S9 and S10).[55] Amorphous configurations were constructed from five polymer chains with degree of polymerization of 28 via random placement using CHARMM,[56] with further details of the build procedure in supplemental experimental procedures. Following a multi-step equilibration, temperatures from −173°C to 373°C (100–550 K) were simulated in 20 K increments (5 ns of MD in the NPT ensemble for each temperature in NAMD),[57] enabling analysis over a broad temperature range spanning from well above to well below the experimental T_g values (Figure S7 and Table S11). An analogous suite of simulations (from 550 K to 250 K in 10 K increments) facilitated analysis of the dynamics of each polymer system with finer temperature resolution.

We utilized this latter suite of simulations to examine the dynamics for every backbone dihedral for the three polymers (Figure 5A). "Dihedral 1" is centered upon the diacid region whereas "dihedral 8" is likewise centered upon the diamine region; other backbone dihedrals not labeled are redundant with these in nylon-6,6. We chose these to quantify the effect of the ketone moiety and its position on the

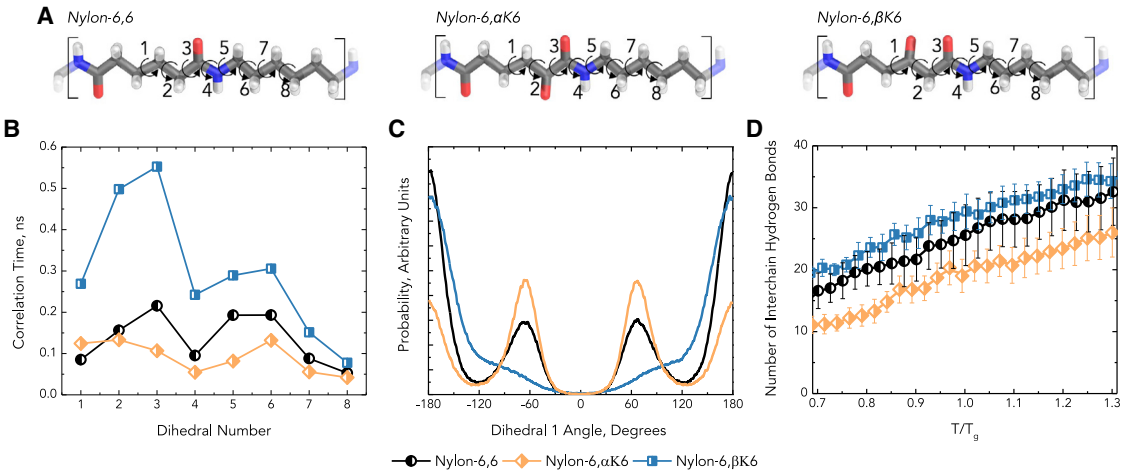

Figure 5. Results from molecular dynamics simulations to understand β-ketone rigidity

Molecular dynamics (MD) simulations suggest increased backbone rigidity in nylon-6,βK6.

(A) Naming convention for the eight backbone dihedrals in the 6,6 suite of nylons presented in (B).

(B) Correlation time for each backbone dihedral defined in (A), demonstrating slower dynamics in nylon-6,βK6.

(C) Probability distribution for dihedral 1 (defined in A), demonstrating that this dihedral in nylon-6,βK6 is "locked" into a single conformation, in contrast to nylon-6,6 and nylon-6,αK6.

(D) Average number of interchain hydrogen bonds as a function of temperature (scaled by T_g in kelvin); error bars are the SD over the course of the 4 ns of data taken at each temperature. Increased interchain hydrogen bonding is observed when ketone is present in nylon-6,6 at the β, but not the α, position.

ns, nanoseconds; T_g, glass transition temperature.

intrachain polymer dynamics. From the MD trajectories, we calculated the correlation time for each dihedral, as defined in supplemental information. At 207°C (480 K, above the experimental T_g for all polymers considered), marked increases in the correlation times (compared with nylon-6,6) of dihedrals near the ketone were observed in nylon-6,βK6 but not for nylon-6,αK6 (Figure 5B). Indeed, correlation times for all backbone dihedrals are increased for nylon-6,βK6, with those in the diacid region and near the peptide bond exhibiting the highest magnitude (dihedrals 1 through 4 in Figures 5A and 5B). Correlation times for dihedrals 1 and 2 are more than three times higher for nylon-6,βK6 than for nylon-6,6; dihedrals 3 and 4 are about 2.5 times higher. Analysis of the full temperature range of the MD simulations reveals that this trend of prolonged correlation times holds at all temperatures studied above the T_g (Figure S7).

For select dihedrals, the increased correlation times can be correlated with changes in the probability distributions of dihedral angles sampled. Figure 5C provides the probability distribution for the central dihedral of the diacid region ("dihedral 1"), in which nylon-6,βK6 samples around a single dihedral value, whereas nylon-6,6 and nylon-6,αK6 sample three different values corresponding to the typical *trans* and *gauche* positions. (In other cases, e.g., "dihedral 2" and "dihedral 3", the sampled dihedral ranges are less substantially different.) It is possible that increased rigidity centered around one backbone bond can propagate down the chain, considering that backbone rotations generally occur in pairs.

In addition to increased stiffness of the polymer backbone due to the β-ketone, our modeling also predicted that this moiety affects the interactions between polymer chains. Hydrogen bonding with adjacent polymer chains is increased with the ketone present in the β (but not the α) position (Figure 5D). In fact, in the case of nylon-6,αK6, fewer interchain hydrogen bonds are present than in nylon-6,6. In

Figure 5D, the average number of hydrogen bonds formed between chains is shown as a function of the dimensionless temperature—the absolute temperature scaled by T_g as estimated by MD (for procedure and results, see supplemental information). Scaling each temperature by the predicted T_g allows examination of the effect on hydrogen bonding in each polymer regime (glassy and rubbery); this analysis reveals that the enhanced interchain hydrogen bonding is consistently seen in all regimes: below, near, and above the predicted T_g. Overall, the MD simulation results suggest that the molecular basis for the enhanced thermal properties of nylon-6,βK6, namely the increase in T_g, can be traced to increased rigidity of the polymer backbone due to the β-ketone group.

Techno-economic analysis and supply-chain modeling of nylons

To identify the key drivers for economics, energy use, and GHG emissions associated with monomer production, we conducted TEA and supply-chain modeling conducted for a hypothetical βKA production plant (Figure 6A). These results provide an estimate of the minimum selling price (MSP) of βKA relative to adipic acid and HMDA (Figure 6B), capital expenses (CapEx, Figure 6C) and the annual operating expenses (OpEx, Figure 6D) as a function of process sections, and the associated supply-chain level energy and GHG emissions.

For the base case commercial plant design, we assumed a βKA molar yield of 40% (per mole of glucose) with a product titer reaching 90 g/L (a productivity of 1 g/L/h). We modeled a biochemical facility that uses bubble columns and a glucose feedstock to produce 102.5 kilotons of βKA/year. This scale represents ~14% of the combined annual nylon-6,6 and nylon-6 market in the United States and 2% of the global market.[58] For reference, this is equivalent to ~two-thirds of the INVISTA facility in Camden, South Carolina producing nylon-6,6. Interestingly, nylon-6,6 consumes 85% of the total adipic acid demand. Selection of this plant size also enables comparison with previously published work on adipic acid production.[39]

Post biological cultivation, it is assumed that 95% of the βKA can be recovered via simulated moving bed chromatography, while the sodium sulfate salt produced is sent to waste disposal. Simulated moving beds were selected because of their applicability to biomass-derived monomers (e.g., lactic acid), the propensity for βKA to decarboxylate, and the inability to separate βKA via crystallization.[59,60] Operating conditions and other pertinent information are outlined in supplemental experimental procedures. Tables S12–S15 provide the biological cultivation, equipment assumptions, and material costs, and Table S16 provides key financial parameters for discounted cash flow analysis.

For the base case, the CapEx was estimated to be US$116 MM while the annual OpEx would be $168 MM, resulting in a βKA MSP of $1.94/kg. These costs align with the previous analysis of MA with a similar plant capacity, which enables direct MSP comparisons.[39] The largest driver of CapEx is the cost associated with the biological cultivation section, which includes the bubble column bioreactors, seed trains, and compressors, accounting for 85.8% of the cost (Figure 6C). To achieve the target product titer and plant throughput, the cultivation was assumed to run for 90 h (with an additional 10 h turnaround time), which would require installing multiple parallel units. The remainder of the CapEx is for separations, where the simulated moving bed columns account for 10.2% of the cost.

Similar trends are observed in the OpEx (Figure 6D), of which the biological cultivation section and the seed train represents 70% of the cost, at approximately $107

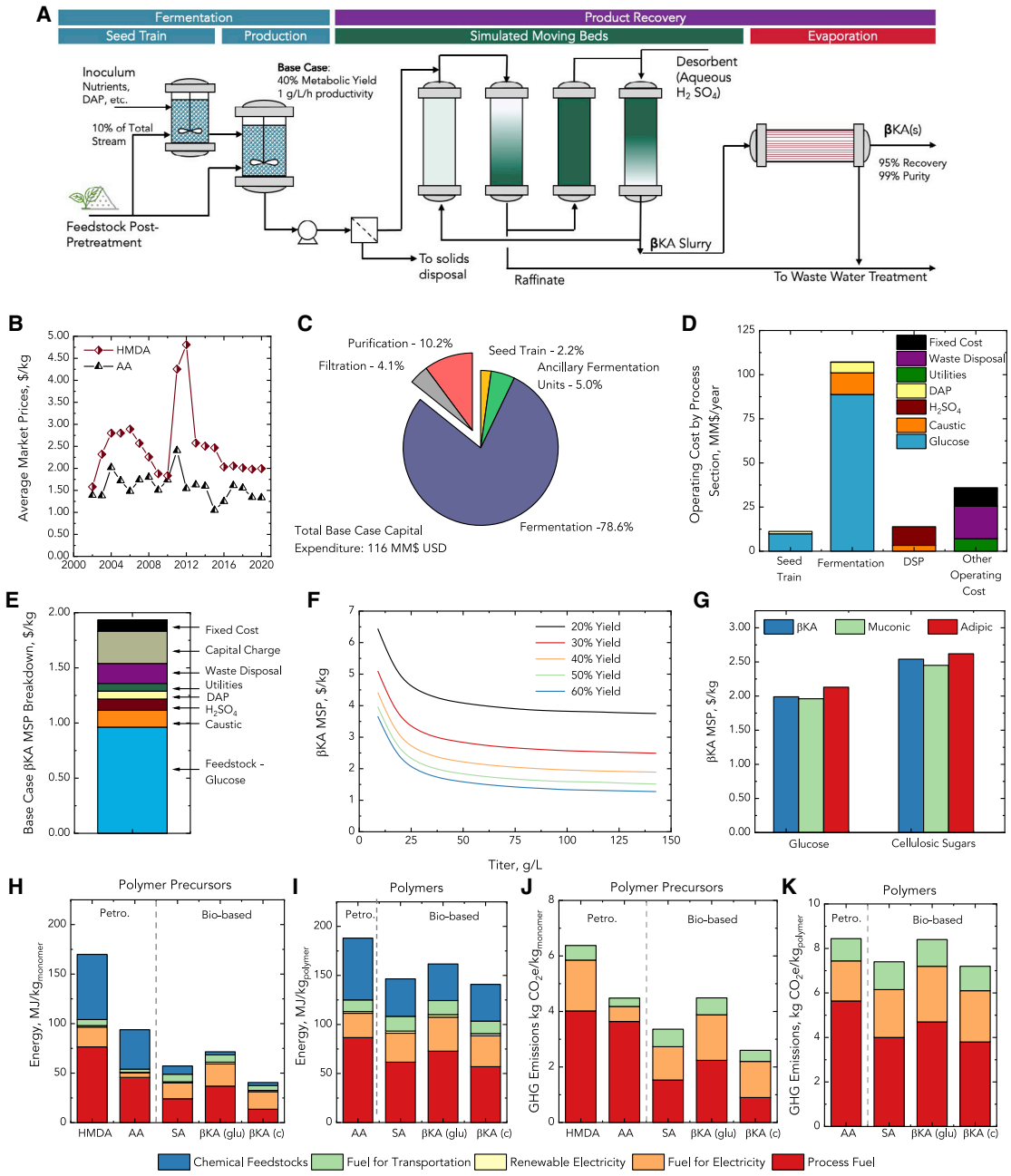

Figure 6. Economic and supply-chain analysis of βKA and subsequent polymers

(A) Process flow diagram to produce βKA.

(B) Historic prices of adipic acid and hexamethylene diamine.

(C) Capital expenses (CapEx) breakdown by process section for the base case.

(D) Operating expenses (OpEx) as a function of process section for the base case.

(E) Minimum selling price (MSP) for βKA broken down into the factors affecting cost.

(F–K) Sensitivities of the MSP of βKA as a function of (F) glucose-based sugar yield and titer, as well as (G) feedstock type. MFI results including (H and I) the supply-chain energy and (J and K) GHG emissions of the production of the nylon precursors and homopolymer nylons from this work. Tables S17–S20 provide the numerical values for these data.

MSP, minimum selling price; HMDA, hexamethylene diamine; AA, adipic acid; DAP, diammonium phosphate; DSP, downstream processing; SA, sebacic acid; βKA(glu.), β-ketoadipic acid from glucose; βKA(C), β-ketoadipic acid from cellulosic sugars.

MM/year and $11 MM/year, respectively. Feedstock cost is a major driver at $0.27/kg. Downstream separation costs include use of sulfuric acid to protonate βKA and caustic to regenerate the simulated moving beds, comprising 8% of the OpEx, while "other operating costs" contribute 21%, including waste disposal, fixed costs, and utilities.

Figure 6E shows the primary contributions to the MSP for βKA using a discounted cash flow method applied to the CapEx and OpEx. The greatest contributor to cost is glucose as a feedstock, contributing $0.93/kg or 48% of the cost. The capital charge contributes $0.29/kg, and the use of acid and caustic contributes $0.26/kg. The remainder of costs is associated with ancillary categories such as utilities and waste disposal.

Several of these cost factors were examined in sensitivity analysis. Product titer and metabolic yield were examined to identify potential improvements to reduce the cost associated with fermentations (Figure 6F). Base industrial design discussed here assumed metabolic yield of 40% per mole of glucose and an average residence time of 90 h, such that the final product titer is 90 g/L. Examining the effect of titer first, the βKA selling price increases with decreasing titers, especially below 40 g/L as downstream processing becomes more costly. Above 60 g/L, the impact of titer gains on MSP diminishes. Metabolic yield also has a substantial effect on MSP as a function of titer and productivity. At a molar yield of 20%, half the yield of the base case, the MSP increases by 100% while at a metabolic yield of 50%, the MSP is reduced by 19%. Additional factors, such as plant size and bubble column reactor costs, that affect the economics are shown in Figure S8.

Since glucose is a key cost driver, cellulosic sugars were investigated as an alternative substrate. Figure S9 provides a comparison of MSP as a function of feedstock cost. Additionally, the cost of bio-derived βKA was also compared with the cost of MA and adipic acid from previous work.[39] The feedstock comparison was conducted at the same productivity, yield, and separation efficiency as the base case (Figure 6G). Cost differences between βKA, adipic acid, and MA are minimal (±$0.10/kg), with MA estimated to be the lowest-cost monomer to produce owing to its simpler separations (i.e., crystallization) while adipic acid is estimated to have the highest MSP, as it is modeled via hydrogenation of MA.[19,26,61–63] Cellulosic sugars were estimated to exhibit the highest MSP due to the higher feedstock cost.

Supply-chain modeling to produce both the monomers and nylon polymers was conducted with MFI to estimate supply-chain energy intensity (Figures 6H and 6I) and GHG emissions (Figures 6J and 6K). Specifically, bio-based βKA from glucose and cellulosic sugars, bio-based sebacic acid from castor oil, petroleum-derived adipic acid and HMDA, and the nylons from the salt-based polymerization of petroleum-derived HMDA with each diacid were modeled. For adipic acid and sebacic acid, existing commercial processes were modeled, and βKA production was modeled using the base case above. Details on MFI can be found in supplemental information, in the original report,[43] or in other works that focus on the use of MFI for polymers.[30,58] MFI does not account for CO_2 credits from the growth of the bio-based feedstocks, such that these potential credits are not included in Figure 6; GHG emissions credits are estimated in Figure 7.

In all cases examined, the βKA supply chain was estimated to require less energy than that of petroleum-derived adipic acid (34% and 63% less energy on a per-kg basis for glucose and cellulosic sugars feedstocks, respectively). βKA from glucose is

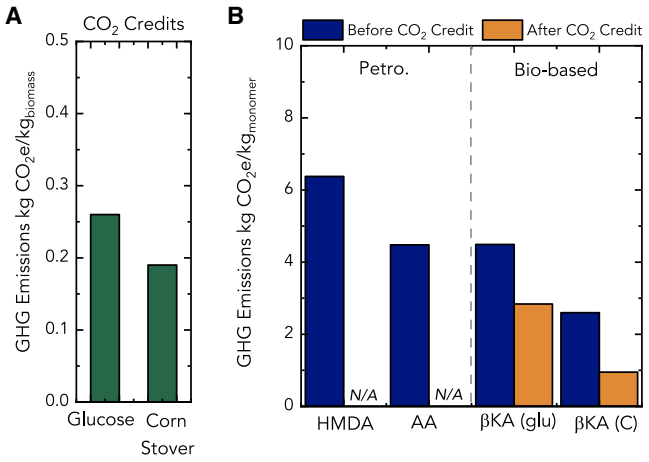

Figure 7. CO_2 offset estimates from the use of bio-derived feedstocks

(A) CO_2 credits for glucose and cellulose feedstocks for βKA production on a mass basis.

(B) Supply-chain GHG emissions for monomers before and after CO_2 credits.

estimated to generate approximately the same level of supply-chain GHG emissions as adipic acid, whereas βKA from cellulosic sugars produces 42% less CO_2e on a per-kg basis due to relatively lower fossil energy requirements for producing the feedstock (Figure 6J). Glucose produced by wet milling of corn requires natural gas and electricity inputs, whereas the modeled process for cellulosic sugars production has no natural gas input and exhibits a net negative electricity requirement (i.e., an electricity credit) from lignin combustion. Compared with sebacic acid, βKA from glucose was estimated to require 25% more supply-chain energy and generate 35% more supply-chain GHG emissions, while βKA from cellulosic sugars was estimated to require 29% less supply-chain energy and generate 22% less supply-chain GHG emissions compared with sebacic acid. Further supply-chain energy and GHG emission reductions may be possible with alternative separation schemes. As an example, the separation of βKA, which uses a simulated moving bed, results in 10 MJ/kg higher supply-chain energy than MA, which employs crystallization (Figure S10).

Supply-chain impacts are lessened when considering the polymer products instead of solely the monomer production, due to the use of fossil-derived HMDA in all scenarios. HMDA, which is modeled as butadiene hydrocyanation, constitutes between 40% and 50% of the polymer mass and exhibits the highest supply-chain energy and GHG emissions impacts compared with any other precursor in this study.

As noted above, MFI does not account for CO_2 sequestered during biomass cultivation, resulting in a potential underestimate of the GHG reductions associated with the production of bio-derived monomers and polymers. We provide an initial estimate of the CO_2 offset for each feedstock on a per-kg basis in Figure 7. On a per-kg of biomass/feedstock basis, glucose- and cellulosic sugar-derived βKA have offsets of 0.26 and 0.19 kg CO_2e/kg, respectively based on calculations with inputs from the Ecoinvent database (Figure 7A).[64] When these estimates are applied to the production of βKA on a per-mass basis, which calculates the amount of carbon in the final product, the estimated GHG emissions are reduced by 1.65 kg CO_2e/kg for both glucose- and cellulosic-derived βKA (Figure 7B). Relative to adipic acid production, this estimate would result in a 37% and 79% reduction in GHG emissions for glucose and cellulosic sugar-derived βKA, respectively. Finally, even

though CO_2 is sequestered in the growth of bio-based feedstocks, there are no estimated reductions to the supply-chain energy; thus, the estimates in Figures 6H and 6I would not change.

DISCUSSION

This work demonstrates that unique chemical functionality from bio-derived compounds can enable enhanced performance when incorporated into polymers. Specifically, we showed that β-ketones enable rigidity in nylon by limiting motion across multiple bonds. The results presented here suggest that β-ketones could similarly enhance performance when incorporated into other polymers. In addition to superior polymer properties, βKA production was estimated to exhibit both lower energy requirements and GHG emissions relative to production of fossil carbon-based analogs. A potential modification of the process (which was not analyzed in this work) would be a recovery system for the waste sodium sulfate salt; such a co-product could lead to an additional economic, energy, and GHG credits, depending on the intensity of the recovery process. Additionally, while this work features several benefits of biological diacid production, it also highlights the need for bio-based HMDA production, given that this monomer today consumes nearly double the supply-chain energy compared with adipic acid. Bio-based processes[65,66] offer the potential to access diamines through alternative routes.

The strain developed here leverages substantial learning from engineering of *P. putida* for MA production, which is an intermediate in the βKA pathway.[39,42] As noted above, the current strain performance in terms of yield and titer modeled as the base case in the TEA efforts have not yet been achieved experimentally. In addition, SN301 is not able to utilize xylose for βKA production. Going forward, we intend to apply similar engineering strategies for xylose and arabinose utilization to βKA, as reported previously,[67,68] to further conversion to βKA. By leveraging these modifications for βKA production, we anticipate being able to achieve the yield, titer, and productivity targets modeled in the TEA base case process.

As noted above, nylon-6,10 produced with bio-derived sebacic acid exhibits lower water permeability and uptake than nylon-6,6, which is attributed to the longer aliphatic region in sebacic acid.[50,65,69,70] However, sebacic acid is currently synthesized via catalytic conversion of castor oil,[53,71–73] in which ricin can be a toxic by-product. Given growing consumer concerns over health risks associated with plastics production and end use, processes with lower associated health risks are of interest.[74] Bioconversion strategies can also result in safer processes, as metabolic engineering can also be leveraged to tolerate and/or convert toxic by-products (e.g., phenols) to benign products.[75–78] Moreover, while sebacic acid offers performance advantages through the longer alkyl chain in its backbone, the performance advantages for βKA can be attributed to the β-ketone in its backbone, as shown by experiment and simulation. This enhanced rigidity, when compared with its aliphatic counterpart, leads to an increase in T_g. Similar enhanced performance and rigidity have been previously demonstrated for ketones, such as with γ-ketocaprolactone (γCL) compared with caprolactone (CL).[79] The homopolymers of CL and γCL feature T_g values of −50°C and 37°C, respectively. Latere et al. attribute the increased T_g to the γ-ketone and further demonstrate that the γ-ketone increases the T_m of the caprolactone through intermolecular interactions.[79] The behavior of the ketone in the polymer backbone is also akin to that of polyketones, which are rigid thermoplastics known for their high crystallinities and low permeabilities.[80] Due to the bifunctionality of βKA, it can be introduced into the

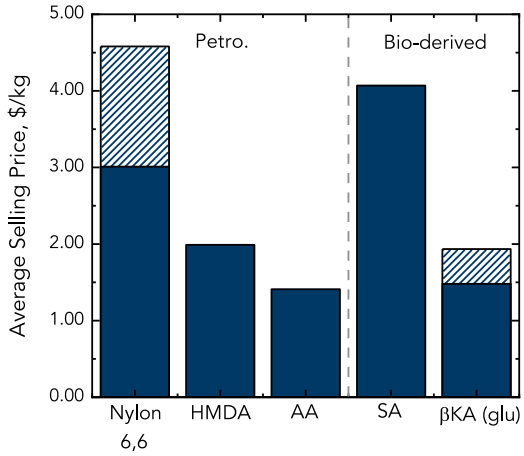

Figure 8. Comparison of selling price of nylon-6,6 and various precursors

Nylon-6,6 can range in selling price from $3.01/kg (solid bar) to $4.58/kg (shaded bar) depending on quality and application. The cost of the nylon exceeds the cost of its inputs (hexamethylene diamine [HMDA] and adipic acid [AA]). Results from techno-economic analysis indicate that βKA could have a selling price ranging from $1.48/kg for higher productivity strains (solid bar) to $1.94/kg for the base case (shaded bar). Sebacic acid (SA) cost exceeds the expected price range for βKA.

backbones of other polymers, such as polyesters or other nylons, to potentially impart similar property enhancements.

The improved performance of the βKA-derived nylons means that the analysis presented in this study comparing their economic and environmental impacts with those of conventional nylons carries an important caveat. The functional unit basis of comparison (e.g., per unit mass of polymer), while straightforward to understand, assumes that the same amount of the βKA-derived nylon material would be needed to achieve a similar function and lifetime when compared with conventional products. Perhaps a polymer with superior properties would require relatively less material or have a longer lifetime than the conventional polymers it is substituting. Adjusting the analysis to reflect such a scenario, however, would then require an assumption of the final application, and this was not pursued here. Therefore, we present the results, conservatively, on a per-unit mass basis, and there may be additional benefits for βKA-based nylons warranting further investigation.

Nylons are ideal for performance-advantaged bioproducts, as they are typically classified as engineering thermoplastics. Due to their robust thermomechanical properties, engineering thermoplastics are typically used in applications that demand a higher selling price than commodity plastics, such as polyethylene, polypropylene, and polystyrene, and can demand different prices depending on their grade within the same polymer formulation (e.g., nylon-6,6). At the time of writing, higher grades of nylons (e.g., nylons with comonomers, tailored molecular weights, additives, or reinforcements that result in greater performance) sell for $4.58/kg compared with $3.01/kg for lower grades, an 80% price differential (Figure 8) (http://www.plasticsnews.com/resin/commodity-thermoplastics/current-pricing). The market price for high-purity sebacic acid for nylon-6,10 is $4.07/kg (https://www.icis.com/explore/resources/news/2003/01/17/188312/a-dramatic-shift-for-us-sebacic-acid) compared with $1.71/kg for adipic acid. Although the current price for sebacic acid is partially due to production shortages, the performance advantages of nylon-6,10 also warrant a higher price. βKA could potentially sell for $1.95/kg in the base case at 40% metabolic yield and 1 g/L/h productivity from glucose (or a 90 g/L titer at a 90 h

residence time), making it potentially competitive with sebacic acid. TEA also indicates that further strain engineering and process optimization to achieve a yield of 50% and a productivity of 1.6 g/L/h could further reduce the βKA selling price to $1.48/kg. Thus, the potential of βKA to supplement or replace sebacic acid, coupled with the continual search for adipic acid replacements,[81] could ultimately enable eventual market adoption.

EXPERIMENTAL PROCEDURES

Resource availability

Lead contact

Further information and requests for resources and reagents should be directed to and will be fulfilled by the lead contact, Gregg T. Beckham (gregg.beckham@nrel.gov).

Materials availability

All data needed to evaluate the conclusions in the paper are present in the paper and/or the supplemental information.

Data and code availability

Aspen Plus is proprietary software that can be purchased by individual users. MFI is a publicly available tool and is accessible at mfitool.nrel.gov.

Materials and methods

All experimental procedures, materials, and methods for this work are provided in supplemental experimental procedures. This includes additional details on all aspects of the study, including materials, analytical development, plasmids and bacterial strain construction, polymer characterization, MD force fields and methods, techno-economic model development, and tabular data for numerical results shown in the figures. Unless otherwise noted, reagents were purchased from Sigma-Aldrich. The βKA used in this work was exclusively produced from biological cultivations as described in the discussion and supplemental information.

SUPPLEMENTAL INFORMATION

Supplemental information can be found online at https://doi.org/10.1016/j.xcrp.2022.100840.

ACKNOWLEDGMENTS

This work was authored by the National Renewable Energy Laboratory, operated by the Alliance for Sustainable Energy for the US Department of Energy (DOE), under contract no. DE-AC36-08GO28308. Funding was provided by the US DOE Office of Energy Efficiency and Renewable Energy Bioenergy Technologies Office, including via the Agile BioFoundry, which funded the metabolic engineering and bioprocess development components of this work. Computer time was provided by the National Renewable Energy Laboratory Computational Sciences Center supported by the DOE Office of EERE under contract number DE-AC36-08GO28308. We thank Jay Fitzgerald and Gayle Bentley at the DOE and members of the Agile BioFoundry for helpful discussions. The authors thank Peter St. John for his assistance in preparing Figure 2 and Heather Mayes for discussion on the MD simulations.

AUTHOR CONTRIBUTIONS

Funding acquisition, G.T.B. and M.F.C.; conceptualization, G.T.B., N.A.R., C.W.J., and D.S.; methodology, N.A.R., S.F.N., B.C.K., B.A.B., A.S., S.R.N., C.W.J., D.S.,

M.F.C., and G.T.B.; investigation, N.A.R., S.F.N., B.C.K., B.A.B., A.S., S.R.N., C.P.K., G.P.C., and K.J.R.; resources, S.R.N., C.P.K., K.J.R., C.W.J., and D.S.; supervision, A.C.C., C.W.J., D.S., M.F.C., and G.T.B.; visualization, N.A.R., B.C.K., and D.S.; writing – original draft, N.A.R., S.F.N., B.C.K., B.A.B., and A.S.; writing – review and editing, G.T.B. and N.A.R.

DECLARATION OF INTERESTS

N.A.R. and G.T.B. hold multiple patents and have filed multiple patent applications on production of performance-advantaged polymers from βKA (US patent number 10,662,289 and US patent application number 20,210,221,945). S.F.N., C.W.J., and G.T.B. hold patents and have filed patent applications on βKA-producing strains (US patent number 10,253,338). G.T.B. is a member of the *Cell Reports Physical Science* Editorial Advisory Board. All other authors declare no competing interests.

INCLUSION AND DIVERSITY

One or more of the authors of this paper self-identifies as an underrepresented ethnic minority in science. One or more of the authors of this paper self-identifies as a member of the LGBTQ+ community. While citing references scientifically relevant for this work, we also actively worked to promote gender balance in our reference list.

Received: January 9, 2022
Revised: February 16, 2022
Accepted: March 14, 2022
Published: April 5, 2022

REFERENCES

1. Gross, R.A., and Kalra, B. (2002). Biodegradable polymers for the environment. Science *297*, 803–807.
2. Ragauskas, A.J., Williams, C.K., Davison, B.H., Britovsek, G., Cairney, J., Eckert, C.A., Frederick, W.J., Hallett, J.P., Leak, D.J., Liotta, C.L., et al. (2006). The path forward for biofuels and biomaterials. Science *311*, 484–489.
3. Williams, C.K., and Hillmyer, M.A. (2008). Polymers from renewable resources: a perspective for a special issue of polymer reviews. Polym. Rev. *48*, 1–10.
4. Tuck, C.O., Pérez, E., Horváth, I.T., Sheldon, R.A., and Poliakoff, M. (2012). Valorization of biomass: deriving more value from waste. Science *337*, 695–699.
5. Zhu, Y., Romain, C., and Williams, C.K. (2016). Sustainable polymers from renewable resources. Nature *540*, 354–362.
6. Nikolau, B.J., Perera, M.A.D.N., Brachova, L., and Shanks, B. (2008). Platform biochemicals for a biorenewable chemical industry. Plant J. *54*, 536–545.
7. Schwartz, T.J., O'Neill, B.J., Shanks, B.H., and Dumesic, J.A. (2014). Bridging the chemical and biological catalysis gap: challenges and outlooks for producing sustainable chemicals. ACS Catal. *4*, 2060–2069.
8. Shanks, B.H., and Keeling, P.L. (2017). Bioprivileged molecules: creating value from biomass. Green. Chem. *19*, 3177–3185.
9. Huo, J., and Shanks, B.H. (2020). Bioprivileged molecules: integrating biological and chemical catalysis for biomass conversion. Annu. Rev. Chem. Biomol. Eng. *11*, 63–85.
10. Fitzgerald, N.D. (2017). Chemistry challenges to enable a sustainable bioeconomy. Nat. Rev. Chem. *1*, 1–3.
11. Fitzgerald, N.D., and Bailey, A. (2018). Moving beyond Drop-In Replacements: Performance Advantaged Biobased Chemicals (US Department of Energy Office of Energy Efficiency and Renewable Energy Bioenergy Technologies Office).
12. Cywar, R.M., Rorrer, N.A., Hoyt, C.B., Beckham, G.T., and Chen, E.Y.-X. (2021). Bio-based polymers with performance-advantaged properties. Nat. Rev. Mater. *7*, 83–103.
13. Lee, S.Y., Kim, H.U., Chae, T.U., Cho, J.S., Kim, J.W., Shin, J.H., Kim, D.I., Ko, Y.-S., Jang, W.D., and Jang, Y.-S. (2019). A comprehensive metabolic map for production of bio-based chemicals. Nat. Catal. *2*, 18–33.
14. Hermann, B.G., Blok, K., and Patel, M.K. (2007). Producing bio-based bulk chemicals using industrial biotechnology saves energy and combats climate change. Environ. Sci. Technol. *41*, 7915–7921.
15. Sheldon, R.A. (2014). Green and sustainable manufacture of chemicals from biomass: state of the art. Green. Chem. *16*, 950–963.
16. Gallezot, P. (2007). Catalytic routes from renewables to fine chemicals. Catal. Today *121*, 76–91.
17. Jang, Y.-S., Kim, B., Shin, J.H., Choi, Y.J., Choi, S., Song, C.W., Lee, J., Park, H.G., and Lee, S.Y. (2012). Bio-based production of C2-C6 platform chemicals. Biotechnol. Bioeng. *109*, 2437–2459.
18. Schwartz, T.J., Shanks, B.H., and Dumesic, J.A. (2016). Coupling chemical and biological catalysis: a flexible paradigm for producing biobased chemicals. Curr. Opin. Biotechnol. *38*, 54–62.
19. Draths, K.M., and Frost, J.W. (1994). Environmentally compatible synthesis of adipic acid from D-glucose. J. Am. Chem. Soc. *116*, 399–400.
20. Frost, J.W., Miermont, A., Schweitzer, D., and Bui, V. (2013). Preparation of *Trans*, *Trans* Muconic Acid and *Trans*, *Trans* Muconates, Patent Number: US8426639.
21. Matthiesen, J.E., Suástegui, M., Wu, Y., Viswanathan, M., Qu, Y., Cao, M., Rodriguez-Quiroz, N., Okerlund, A., Kraus, G., Raman, D.R., et al. (2016). Electrochemical conversion of biologically produced muconic acid: key considerations for scale-up and corresponding technoeconomic analysis. ACS Sustain. Chem. Eng. *4*, 7098–7109.
22. Becker, J., Kuhl, M., Kohlstedt, M., Starck, S., and Wittmann, C. (2018). Metabolic engineering of Corynebacterium glutamicum

for the production of *cis, cis*-muconic acid from lignin. Microb. Cell Factories *17*, 115.

23. Matthiesen, J.E., Carraher, J.M., Vasiliu, M., Dixon, D.A., and Tessonnier, J.-P. (2016). Electrochemical conversion of muconic acid to biobased diacid monomers. ACS Sustain. Chem. Eng. *4*, 3575–3585.

24. Xie, N.Z., Liang, H., Huang, R.B., and Xu, P. (2014). Biotechnological production of muconic acid: current status and future prospects. Biotechnol. Adv. *32*, 615–622.

25. Lu, R., Lu, F., Chen, J., Yu, W., Huang, Q., Zhang, J., and Xu, J. (2016). Production of diethyl terephthalate from biomass-derived muconic acid. Angew. Chem. Int. Ed. *55*, 249–253.

26. Vardon, D.R., Franden, M.A., Johnson, C.W., Karp, E.M., Guarnieri, M.T., Linger, J.G., Salm, M.J., Strathmann, T.J., and Beckham, G.T. (2015). Adipic acid production from lignin. Energy Environ. Sci. *8*, 617–628.

27. Vardon, D.R., Rorrer, N.A., Salvachua, D., Settle, A.E., Johnson, C.W., Menart, M.J., Cleveland, N.S., Ciesielski, P.N., Steirer, K.X., Dorgan, J., et al. (2016). cis,cis-Muconic acid: separation and catalysis to bio-adipic acid for nylon-6,6 polymerization. Green. Chem. *18*, 3397–3413.

28. Rorrer, N.A., Dorgan, J.R., Vardon, D.R., Martinez, C.R., Yang, Y., and Beckham, G.T. (2016). Renewable unsaturated polyesters from muconic acid. ACS Sustain. Chem. Eng. *4*, 6867–6876.

29. Rorrer, N.A., Vardon, D.R., Dorgan, J.R., Gjersing, E.J., and Beckham, G.T. (2017). Biomass-derived monomers for performance-differentiated fiber reinforced polymer composites. Green. Chem. *19*, 2812–2825.

30. Rorrer, N.A., Nicholson, S., Carpenter, A., Biddy, M.J., Grundl, N.J., and Beckham, G.T. (2019). Combining reclaimed PET with bio-based monomers enables plastics upcycling. Joule *3*, 1006–1027.

31. Carraher, J.M., Pfennig, T., Rao, R.G., Shanks, B.H., and Tessonnier, J.-P. (2017). *Cis , cis* -Muconic acid isomerization and catalytic conversion to biobased cyclic-C 6 -1,4-diacid monomers. Green. Chem. *19*, 3042–3050.

32. Settle, A.E., Berstis, L., Rorrer, N.A., Roman-Leshkóv, Y., Beckham, G.T., Richards, R.M., and Vardon, D.R. (2017). Heterogeneous Diels–Alder catalysis for biomass-derived aromatic compounds. Green. Chem. *19*, 3468–3492.

33. Harwood, C.S., and Parales, R.E. (1996). The β-ketoadipate pathway and the biology of self-identity. Annu. Rev. Microbiol. *50*, 553–590.

34. Salvachúa, D., Karp, E.M., Nimlos, C.T., Vardon, D.R., and Beckham, G.T. (2015). Towards lignin consolidated bioprocessing: simultaneous lignin depolymerization and product generation by bacteria. Green. Chem. *17*, 4951–4967.

35. Beckham, G.T., Johnson, C.W., Karp, E.M., Salvachúa, D., and Vardon, D.R. (2016). Opportunities and challenges in biological lignin valorization. Curr. Opin. Biotechnol. *42*, 40–53.

36. Masai, E., Shinohara, S., Hara, H., Nishikawa, S., Katayama, Y., and Fukuda, M. (1999). Genetic and biochemical characterization of a 2-pyrone-4, 6-dicarboxylic acid hydrolase involved in the protocatechuate 4, 5-cleavage pathway of *Sphingomonas paucimobilis* SYK-6. J. Bacteriol. *181*, 55–62.

37. Mycroft, Z., Gomis, M., Mines, P., Law, P., and Bugg, T.D.H. (2015). Biocatalytic conversion of lignin to aromatic dicarboxylic acids in *Rhodococcus jostii* RHA1 by re-routing aromatic degradation pathways. Green. Chem. *17*, 4974–4979.

38. Okamura-Abe, Y., Abe, T., Nishimura, K., Kawata, Y., Sato-Izawa, K., Otsuka, Y., Nakamura, M., Kajita, S., Masai, E., Sonoki, T., et al. (2016). Beta-ketoadipic acid and muconolactone production from a lignin-related aromatic compound through the protocatechuate 3,4-metabolic pathway. J. Biosci. Bioeng. *121*, 652–658.

39. Johnson, C.W., Salvachúa, D., Rorrer, N.A., Black, B.A., Vardon, D.R., St. John, P.C., Cleveland, N.S., Dominick, G., Elmore, J.R., Grundl, N., et al. (2019). Innovative chemicals and materials from bacterial aromatic catabolic pathways. Joule *3*, 1523–1537.

40. Utomo, R.N.C., Li, W.-J., Tiso, T., Eberlein, C., Doeker, M., Heipieper, H.J., Jupke, A., Wierckx, N., and Blank, L.M. (2020). Defined microbial mixed culture for utilization of polyurethane monomers. ACS Sustain. Chem. Eng. *8*, 17466–17474.

41. Chae, T.U., Ahn, J.H., Ko, Y.-S., Kim, J.W., Lee, J.A., Lee, E.H., and Lee, S.Y. (2020). Metabolic engineering for the production of dicarboxylic acids and diamines. Metab. Eng. *58*, 2–16.

42. Bentley, G.J., Narayanan, N., Jha, R.K., Salvachúa, D., Elmore, J.R., Peabody, G.L., Black, B.A., Ramirez, K., De Capite, A., Michener, W.E., et al. (2020). Engineering glucose metabolism for enhanced muconic acid production in *Pseudomonas putida* KT2440. Metab. Eng. *59*, 64–75.

43. Hanes, R.J., and Carpenter, A. (2017). Evaluating opportunities to improve material and energy impacts in commodity supply chains. Environ. Syst. Decis. *37*, 6–12.

44. Nikel, P.I., Martínez-García, E., and de Lorenzo, V. (2014). Biotechnological domestication of pseudomonads using synthetic biology. Nat. Rev. Microbiol. *12*, 368–379.

45. Nikel, P.I., Chavarría, M., Danchin, A., and de Lorenzo, V. (2016). From dirt to industrial applications: *Pseudomonas putida* as a Synthetic Biology chassis for hosting harsh biochemical reactions. Curr. Opin. Chem. Biol. *34*, 20–29.

46. Nikel, P.I., and de Lorenzo, V. (2018). *Pseudomonas putida* as a functional chassis for industrial biocatalysis: from native biochemistry to trans-metabolism. Metab. Eng. *50*, 142–155.

47. Nikel, P.I., Chavarría, M., Fuhrer, T., Sauer, U., and de Lorenzo, V. (2015). *Pseudomonas putida* kt2440 strain metabolizes glucose through a cycle formed by enzymes of the entner-doudoroff, embden-meyerhof-parnas, and pentose phosphate pathways*. J. Biol. Chem. *290*, 25920–25932.

48. Kikuchi, Y., Tsujimoto, K., and Kurahashi, O. (1997). Mutational analysis of the feedback sites of phenylalanine-sensitive 3-deoxy-D-arabino-heptulosonate-7-phosphate synthase of *Escherichia coli*. Appl. Environ. Microbiol. *63*, 761–762.

49. Daddaoua, A., Krell, T., and Ramos, J.-L. (2009). Regulation of glucose metabolism in Pseudomonas: the phosphorylative branch and entner-doudoroff enzymes are regulated by a repressor containing a sugar isomerase domain. J. Biol. Chem. *284*, 21360–21368.

50. Marchildon, K. (2011). Polyamides – still strong after seventy years. Macromol. React. Eng. *5*, 22–54.

51. Daimon, H., Okitsu, H., and Kumanotani, J. (1975). Glass transition behaviors of random and block copolymers and polymer blends of styrene and cyclododecyl acrylate. I. glass transition temperatures. Polym. J. *7*, 460–466.

52. Bruson, H.A., and Covert, L.W. (1939). Process for Manufacturing Sebacic Acid, Patent Number: US2182056A.

53. Yu, S., Cui, J., Wang, X., Zhong, C., Li, Y., and Yao, J. (2020). Preparation of sebacic acid via alkali fusion of castor oil and its several derivatives. J. Am. Oil Chem. Soc. https://doi.org/10.1002/aocs.12342.

54. Best, R.B., Zhu, X., Shim, J., Lopes, P.E.M., Mittal, J., Feig, M., and MacKerell, A.D. (2012). Optimization of the additive CHARMM all-atom protein force field targeting improved sampling of the backbone φ, ψ and side-chain χ1 and χ2 dihedral angles. J. Chem. Theor. Comput. *8*, 3257–3273.

55. Vanommeslaeghe, K., Hatcher, E., Acharya, C., Kundu, S., Zhong, S., Shim, J., Darian, E., Guvench, O., Lopes, P., Vorobyov, I., et al. (2010). CHARMM general force field: a force field for drug-like molecules compatible with the CHARMM all-atom additive biological force fields. J. Comput. Chem. *31*, 671–690.

56. Brooks, B.R., Brooks, C.L., Mackerell, A.D., Nilsson, L., Petrella, R.J., Roux, B., Won, Y., Archontis, G., Bartels, C., Boresch, S., et al. (2009). CHARMM: the biomolecular simulation program. J. Comput. Chem. *30*, 1545–1614.

57. Phillips, J.C., Braun, R., Wang, W., Gumbart, J., Tajkhorshid, E., Villa, E., Chipot, C., Skeel, R.D., Kalé, L., and Schulten, K. (2005). Scalable molecular dynamics with NAMD. J. Comput. Chem. *26*, 1781–1802.

58. Nicholson, S.R., Rorrer, N.A., Carpenter, A.C., and Beckham, G.T. (2021). Manufacturing energy and greenhouse gas emissions associated with plastics consumption. Joule *5*, 673–686.

59. Huang, H.-J., and Ramaswamy, S. (2013). Overview of biomass conversion processes and separation and purification Technologies in biorefineries. In Separation and Purification Technologies in Biorefineries, S. Ramaswamy, H.-J. Huang, and B.V. Ramarao, eds. (John Wiley & Sons, Ltd), pp. 1–36.

60. Chin, C.Y., and Wang, N.-H.L. (2013). Simulated moving-bed technology for biorefinery applications. In Separation and Purification Technologies in Biorefineries, S. Ramaswamy,

H.-J. Huang, and B.V. Ramarao, eds. (John Wiley & Sons, Ltd), pp. 167–202.

61. Beerthuis, R., Rothenberg, G., and Shiju, N.R. (2015). Catalytic routes towards acrylic acid, adipic acid and ε-caprolactam starting from biorenewables. Green. Chem. *17*, 1341–1361.

62. Deng, Y., Ma, L., and Mao, Y. (2016). Biological production of adipic acid from renewable substrates: current and future methods. Biochem. Eng. J. *105*, 16–26.

63. Corona, A., Biddy, M.J., Vardon, D.R., Birkved, M., Hauschild, M.Z., and Beckham, G.T. (2018). Life cycle assessment of adipic acid production from lignin. Green. Chem. *20*, 3857–3866.

64. Wernet, G., Bauer, C., Steubing, B., Reinhard, J., Moreno-Ruiz, E., and Weidema, B. (2016). The ecoinvent database version 3 (part I): overview and methodology. Int. J. Life Cycle Assess. *21*, 1218–1230.

65. Kind, S., and Wittmann, C. (2011). Bio-based production of the platform chemical 1,5-diaminopentane. Appl. Microbiol. Biotechnol. *91*, 1287–1296.

66. Karp, E.M., Eaton, T.R., Sànchez i Nogué, V., Vorotnikov, V., Biddy, M.J., Tan, E.C.D., Brandner, D.G., Cywar, R.M., Liu, R., Manker, L.P., et al. (2017). Renewable acrylonitrile production. Science *358*, 1307–1310.

67. Dvořák, P., and de Lorenzo, V. (2018). Refactoring the upper sugar metabolism of *Pseudomonas putida* for co-utilization of cellobiose, xylose, and glucose. Metab. Eng. *48*, 94–108.

68. Elmore, J.R., Dexter, G.N., Salvachúa, D., O'Brien, M., Klingeman, D.M., Gorday, K., Michener, J.K., Peterson, D.J., Beckham, G.T., and Guss, A.M. (2020). Engineered *Pseudomonas putida* simultaneously catabolizes five major components of corn stover lignocellulose: glucose, xylose, arabinose, p-coumaric acid, and acetic acid. Metab. Eng. *62*, 62–71.

69. Winnacker, M., and Rieger, B. (2016). Biobased polyamides: recent advances in basic and applied research. Macromol. Rapid Commun. *37*, 1391–1413.

70. Radzik, P., Leszczyńska, A., and Pielichowski, K. (2020). Modern biopolyamide-based materials: synthesis and modification. Polym. Bull. *77*, 501–528.

71. Dytham, R.A., and Weedon, B.C.L. (1960). Organic reactions in strong alkalis-III: fission of keto- and hydroxy-acids. Tetrahedron *8*, 246–260.

72. Naughton, F.C. (1974). Production, chemistry, and commercial applications of various chemicals from castor oil. J. Am. Oil Chem. Soc. *51*, 65–71.

73. Ogunniyi, D.S. (2006). Castor oil: a vital industrial raw material. Bioresour. Technol. *97*, 1086–1091.

74. Halden, R.U. (2010). Plastics and health risks. Annu. Rev. Public Health *31*, 179–194.

75. Franden, M.A., Javakody, L., Li, W.J., Blank, L., Klebensberger, J., Wierckx, N., and Beckham, G.T. (2018). Engineering *Pseudomonas putida* KT2440 for efficient ethylene glycol utilization. Metab. Eng. *48*, 197–207.

76. Jayakody, L.N., Johnson, C.W., Whitham, J.M., Giannone, R.J., Black, B.A., Cleveland, N.S., Klingeman, D.M., Michener, W.E., Olstad, J.L., Vardon, D.R., et al. (2018). Thermochemical wastewater valorization via enhanced microbial toxicity tolerance. Energy Environ. Sci. *11*, 1625–1638.

77. Henson, W.R., Meyers, A.W., Jayakody, L.N., DeCapite, A., Black, B.A., Michener, W.E., Johnson, C.W., and Beckham, G.T. (2021). Biological upgrading of pyrolysis-derived wastewater: engineering *Pseudomonas putida* for alkylphenol, furfural, and acetone catabolism and (methyl)muconic acid production. Metab. Eng. *68*, 14–25.

78. Borchert, A.J., Henson, W.R., and Beckham, G.T. (2022). Challenges and opportunities in biological funneling of heterogeneous and toxic substrates beyond lignin. Curr. Opin. Biotechnol. *73*, 1–13.

79. Latere, J.-P., Lecomte, P., Dubois, P., and Jérôme, R. (2002). 2-Oxepane-1,5-dione: a precursor of a novel class of versatile semicrystalline biodegradable (co)polyesters. Macromolecules *35*, 7857–7859.

80. Holt, G.A., Jr., and Spruiell, J.E. (2002). Melting and crystallization behavior of aliphatic polyketones. J. Appl. Polym. Sci. *83*, 2124–2142.

81. Tiso, T., Winter, B., Wei, R., Hee, J., de Witt, J., Wierckx, N., Quicker, P., Bornscheuer, U.T., Bardow, A., Nogales, J., et al. (2021). The metabolic potential of plastics as biotechnological carbon sources – review and targets for the future. Metab. Eng. https://doi.org/10.1016/j.ymben.2021.12.006.